human reproduction

ORIGINAL ARTICLE *Reproductive biology*

A distinctive epigenetic ageing profile in human granulosa cells

K.W. Olsen[1,2,*,†], J. Castillo-Fernandez[3,†], A. Zedeler[4], N.C. Freiesleben[4,5], M. Bungum[6], A.C. Chan[2], A. Cardona[7,10], J.R.B. Perry[7], S.O. Skouby[1,8], R. Borup[2], E.R. Hoffmann[2], G. Kelsey[3,9], and M.L. Grøndahl[1]

[1]Department of Obstetrics and Gynaecology, Department of Reproductive Medicine, Copenhagen University Hospital Herlev, Herlev, Denmark [2]DNRF Center for Chromosome Stability, Department of Cellular and Molecular Medicine, Faculty of Health and Medical Sciences, University of Copenhagen, Copenhagen, Denmark [3]Epigenetics Programme, Babraham Institute, Cambridge, UK [4]Department of Obstetrics and Gynaecology, The Fertility Clinic, Copenhagen University Hospital Hvidovre, Hvidovre, Denmark [5]Stork IVF Clinic A/S Copenhagen, VivaNeo Fertility Clinics, Copenhagen, Denmark [6]Reproductive Medicine Centre, Skåne University Hospital, Malmoe, Sweden [7]Medical Research Council Epidemiology Unit, University of Cambridge Addenbrooke's Hospital, Cambridge, UK [8]Department of Clinical Medicine, Faculty of Health and Medical Sciences, University of Copenhagen, Copenhagen, Denmark [9]Centre for Trophoblast Research, University of Cambridge, Cambridge, UK [10]Department of Genetics, University of Cambridge, Cambridge, UK

*Correspondence address. E-mail: kristina.wendelboe.olsen.01@regionh.dk, kristinawo@hotmail.com

STUDY QUESTION: Does women's age affect the DNA methylation (DNAm) profile differently in mural granulosa cells (MGCs) from other somatic cells?

SUMMARY ANSWER: Accumulation of epimutations by age and a higher number of age-related differentially methylated regions (DMR) in MGCs were found compared to leukocytes from the same woman, suggesting that the MGCs have a distinctive epigenetic profile.

WHAT IS KNOWN ALREADY: The mechanisms underlying the decline in women's fertility from the mid-30s remain to be fully elucidated. The DNAm age of many healthy tissues changes predictably with and follows chronological age, but DNAm age in some reproductive tissues has been shown to depart from chronological age (older: endometrium; younger: cumulus cells, spermatozoa).

STUDY DESIGN, SIZE, DURATION: This study is a multicenter cohort study based on retrospective analysis of prospectively collected data and material derived from healthy women undergoing IVF or ICSI treatment following ovarian stimulation with antagonist protocol. One hundred and nineteen women were included from September 2016 to June 2018 from four clinics in Denmark and Sweden.

PARTICIPANTS/MATERIALS, SETTING, METHODS: Blood samples were obtained from 118 healthy women with varying ovarian reserve status. MGCs were collected from 63 of the 119 women by isolation from pooled follicles immediately after oocyte retrieval. DNA from leukocytes and MGCs was extracted and analysed with a genome-wide methylation array. Data from the methylation array were processed using the ENmix package. Subsequently, DNAm age was calculated using established and tailored age predictors and DMRs were analysed with the DMRcate package.

MAIN RESULTS AND ROLE OF CHANCE: Using established age predictors, DNAm age in MGCs was found to be considerable younger and constant (average: 2.7 years) compared to chronological age (average: 33.9 years). A Granulosa Cell clock able to predict the age of both MGCs (average: 32.4 years) and leukocytes (average: 38.8 years) was successfully developed. MGCs differed from leukocytes in having a higher number of epimutations ($P = 0.003$) but predicted telomere lengths unaffected by age (Pearson's correlation coefficient $= -0.1$, $P = 0.47$). DMRs associated with age (age-DMRs) were identified in MGCs ($n = 335$) and in leukocytes ($n = 1$) with a significant enrichment in MGCs for genes involved in RNA processing (45 genes, $P = 3.96 \times 10^{-08}$) and gene expression (152 genes, $P = 2.3 \times 10^{-06}$). The top age-DMRs included the metastable epiallele *VTRNA2-1*, the DNAm regulator *ZFP57* and the anti-Müllerian hormone (*AMH*) gene. The apparent discordance between different epigenetic measures of age in MGCs suggests that they reflect difference stages in the MGC life cycle.

LARGE SCALE DATA: N/A.

LIMITATIONS, REASONS FOR CAUTION: No gene expression data were available to associate with the epigenetic findings. The MGCs are collected during ovarian stimulation, which may influence DNAm; however, no correlation between FSH dose and number of epimutations was found.

WIDER IMPLICATIONS OF THE FINDINGS: Our findings underline that the somatic compartment of the follicle follows a different methylation trajectory with age than other somatic cells. The higher number of epimutations and age-DMRs in MGCs suggest that their function is affected by age.

Introduction

The most important factor in determining female fertility potential is age. Most countries within the Organisation for Economic Co-operation and Development (OECD) have seen the average age of women at childbirth increase by between 2 and 5 years from 1970 to 2015 (OECD Family Database, 2018). In Denmark in 2018, the average age for women giving birth was 31.0 years, while the age of first-time mothers was 29.3 years; in comparison, in 1968 the figures were 26.5 and 23.1 years, respectively (Statistics Denmark, 2018). This implies an increasing challenge for female fertility followed by an increasing need of assisted reproduction, because both the quantity and quality (the competence to establish an ongoing pregnancy) of oocytes decline with advanced age (Franasiak et al., 2014). Children born after medically assisted reproduction in 2018 represented 9.8% of the Danish birth cohort (The Danish Fertility Society, 2019). While life expectancy has increased substantially over the last century, timing of menopause as well as the age-related decline in reproductive potential have remained unchanged (Baird et al., 2005; Ceylan and Ozerdogan, 2015), although some studies have indicated a small delay in the onset of menopause (Van Noord et al., 1997; Rödström et al., 2003).

During foetal life, oocytes arrested in the pro-phase of first meiosis are laid down in the ovary surrounded by one layer of pre-granulosa cells in the primordial follicles, which comprise the reproductive potential of the girl. In the primordial follicle, the pre-granulosa cells also remain in cell cycle arrest (Scalercio et al., 2015) for up to five decades until activation and subsequent folliculogenesis, a lengthy (6-month) and highly complex process in which the follicles develop and mature. Upon activation, the pre-granulosa cells start proliferating and develop into an estimated 60 million mural granulosa cells (MGCs) (McNatty et al., 1979) crucial for oestrogen production, ovulation of the matured oocyte in metaphase II, followed by luteinization and corpus luteum formation (Dorrington et al., 1975). Follicular atresia affects all stages of folliculogenesis and only a limited number of the original 1–2 million oocytes present in the female ovary at birth remain when a woman reaches the age of 40 years. In addition to this depletion in the ovarian reserve of primordial follicles, the diminishing quality of oocytes including increase in aneuploidy (Franasiak et al., 2014) means that many women completely lose the ability to reproduce by the age of 40 years (Scheffer et al., 2003). The mechanisms involved in the age-associated increase in meiotic errors in human oocytes remain to be fully elucidated. Several hypotheses for the reduced oocyte competence by age have been proposed, for example, the germline bottleneck theory of mutations in mitochondria, which considers that the most competent primordial follicles are selected and activated first, resulting in mitochondrial dysfunction, because of deleterious mutations in the remaining aged oocytes (Bergstrom and Pritchard, 1998). The focus of the present study is the somatic cell compartments of the follicle: the cells that, by bidirectional communication with the oocytes, as well as by delivering nutrients to the oocyte, are crucial for oogenesis throughout folliculogenesis (Eppig, 2001; Gilchrist et al., 2008). It has been suggested, based on data in Rhesus monkeys, that the capacity of pre-granulosa cells to repair double-stranded DNA breaks declines with increasing age (Zhang et al., 2015), as occurs in other somatic tissues with age. Whether granulosa cells age more rapidly than the rest of the body, thereby losing functionality and ability to support oocyte development, is not known.

Recently, it has been found that DNA methylation (DNAm) patterns can be used to predict chronological age with high accuracy. In 2013, Steve Horvath developed a multi-tissue age predictor (epigenetic clock), which is able to estimate age of most tissues and cell types with an accuracy of 3.6 years (Horvath, 2013). The prediction is based on the weighted combination of methylation levels (methylation and demethylation) at 353 specific cytosine–phosphate–guanine (CpG) sites distributed across the genome. These CpG sites were selected out of 21 369 CpG sites measured with the Illumina 27 K and 450 K methylation array platforms and by analysing 7844 non-cancer samples from 82 datasets containing 52 different cell and tissue types (Horvath, 2013). The predicted age, referred to as DNAm age, is considered a biological measure of ageing. When the estimated DNAm age differs from the chronological age, the term 'age acceleration' is used to describe faster or slower rates of ageing (Horvath, 2013). Subsequently, several studies have found such deviations between the DNAm age and the chronological age in various tissue types and individuals (Horvath et al., 2015a; Horvath, et al., 2015b; Sehl et al., 2017). One of the most interesting findings is that accelerated DNAm age in blood is associated with all-cause risk of mortality (Marioni et al., 2015; Perna et al., 2016). Since the development of the multi-tissue age predictor, several more specialized epigenetic clocks have been developed with the aim of measuring different aspects of the ageing process (Weidner et al., 2014; Giuliani et al., 2016; Levine et al., 2018). Telomere length has for more than a decade been proposed to act as a biomarker for ageing (Sanders and Newman 2013) and possible relationship between female fertility and telomere length is debated (Kosebent et al., 2018). Recently, an estimator of telomere length based on DNAm data (DNAmTL) has been developed (Lu et al., 2019).

As the ability to reproduce is highly age-dependent in women, the above findings may have relevance in the understanding of ovarian ageing. A recent study by Morin et al., found that DNAm age of cumulus cells measured with Horvath's multi-tissue clock was substantially younger than chronological age regardless of the age and the response to ovarian stimulation of the women (Morin et al., 2018). The multi-tissue age predictor has been evaluated in other reproductive tissues, e.g. endometrium, in which the predicted age was significantly older compared with chronological age (Olesen et al., 2018), and spermatozoa, in which the predicted age was significantly younger than the chronological age (Horvath, 2013). Moreover, DNAm age acceleration in leukocytes has been associated with reproductive life events such as menarche, puberty, and early menopause (Levine et al., 2016; Simpkin et al., 2017; Binder et al., 2018). However, the predictor

has not been tested in MGCs, the cells supporting the oocytes during follicular growth and maturation, and which also produce the female sex hormones. Very few studies have investigated the DNAm profile of MGCs, studies primarily focusing on differences in the methylome from women with polycystic ovarian syndrome (PCOS) (Qu *et al.*, 2012; Pan *et al.*, 2018; Sagvekar *et al.*, 2019). MGCs are available when oocytes are retrieved in treatments during ART. The aims of the present study were to (i) assess the suitability of the multi-tissue DNAm age predictor and the DNAmTL predictor to MGCs and leukocytes from women undergoing ART and (ii) investigate if DNAm profiles of the two cell types change with age and, if so, whether these changes are shared or tissue-specific.

Materials and Methods

Participants

This study is a multicentre cohort study based on retrospective analysis of prospectively collected data and material derived from healthy women undergoing IVF or ICSI treatment following controlled ovarian stimulation (COS) with GnRH antagonist protocol. Women receiving fertility treatment with either IVF or ICSI from September 2016 to January 2018 at four different clinics (Denmark: Herlev Hospital, Hvidovre Hospital, Stork IVF Clinic; Sweden: Skåne University Hospital) were invited to participate regardless of their age and anti-Müllerian hormone (AMH) level. They were primarily included during their first, second or third stimulation cycle. A total of 119 women were included in the study. Only women with no history of disease such as PCOS, severe endometriosis, dysregulated thyroid disease and severe comorbidity (insulin-dependent diabetes mellitus, non-insulin diabetes mellitus, gastrointestinal-, cardio-vascular-, pulmonary, liver or kidney disease) were asked to consider participation in the study. Seven participants were later diagnosed with PCOS as a secondary cause of infertility and were not excluded from the study.

Treatment protocol

The COS was initiated at Days 2–3 of the menstrual cycle with recombinant FSH (Bemfola®, Gedeon Richter, Denmark; Gonal-f®, Merck-Serono, Denmark; Pergoveris®, Merck-Serono, Denmark) or urine-derived human menopausal gonadotropin (Menopur®, Ferring Pharmaceuticals, Denmark) for 8–12 days, followed by the administration of a GnRH antagonist (Orgalutran®; MSD, Denmark). For the final follicle maturation and ovulation induction recombinant human chorionic gonadotropin (Ovitrelle®; Merck-Serono, Denmark) or a GnRH agonist (Gonapeptyl®; Ferring Pharmaceuticals, Denmark) was administrated when the leading follicles reached a diameter of >16 mm. Oocyte retrieval and collection of the MGCs occurred 36 h later.

Sample collection

Peripheral blood was collected (two 6-mL EDTA tubes) at one of the routine ultrasound scan visits in the clinics before the day of the oocyte retrieval. Within 1 h after collection, the samples were centrifuged at 2000*g* at 4°C for 20 min dividing the blood into three sections: plasma, buffy coat and erythrocytes. The buffy coat containing the leukocytes was transferred to a cryovial (377 267, Nunc™, Thermo Fisher Scientific™, Denmark) and stored at −80°C until analysis. Plasma

were divided into three cryovial tubes (377267, Nunc™, Thermo Fisher Scientific™, Denmark) and stored at −80°C. The erythrocytes were discarded. MGCs were isolated manually immediately after oocyte retrieval: granulosa cell aggregates, free of blood clots, were separated from the follicular fluid with a pipette and transferred to a 10-mL tube containing 3 mL washing solution (10% phosphate-buffered saline (AM9625, Invitrogen™, Thermo Fisher Scientific™, Denmark) + sterile water (1:10) + 1% polyvinyl alcohol (341584, Sigma-Aldrich, Denmark)). The MGC suspension was centrifuged at 300*g* for 10 min, and the sediment (the MGCs) was isolated and transferred to a 0.2-mL tube (AB0620, Thermo Fisher Scientific™, USA), snap frozen in liquid nitrogen, and stored at −80°C until analysis. At the time of isolation, the amount of MGC aggregates were noted (few, medium and numerous). Samples from 63 of the women were categorized medium and numerous, and these were chosen for the analysis to ensure sufficient input of DNA.

DNAm analysis

DNA from the leukocytes (1 mL buffy coat) and MGCs was isolated with the ReliaPrep™ Large Volume HT gDNA Isolation kit (A2751, Promega, Wisconsin, USA) according to the manufacturer's protocol. This was done using the Tecan Freedom EVO®-HSM Workstation. Genome-wide methylation levels were measured using the Illumina Infinium MethylationEPIC BeadChip (Illumina Inc., San Diego, CA) (Illumina, 2015). Five hundred nanograms of DNA per sample was bisulfite-treated by use of the Zymo EZ-96 DNA methylation kit (Zymo Research, Irvine, CA, USA). Thereafter, the samples were hybridized to the arrays (Infinium Methylation EPIC array) according to the manufacturer's protocol. The DNA isolation and generation and management of the Illumina EPIC methylation array data was performed by the Human Genotyping Facility of the Genetic Laboratory of the Department of Internal Medicine, Erasmus MC, the Netherlands.

Methylome data processing

Illumina EPIC array data were processed using the ENmix package (Xu *et al.*, 2016) in R (R Core Team, 2016) to obtain methylation beta-values. Briefly, background correction was performed using the Exponential-Normal mixture distribution (ENmix) method using out-of-band type I probe intensities to model background noise (Xu *et al.*, 2016), dye-bias correction was performed using the Regression on Logarithm of Internal Control probes (RELIC) method (Xu *et al.*, 2017) and probe design bias adjustment was performed by implementing the Regression on Correlated Probes (RCP) method (Niu *et al.*, 2016). Signals with a detection *P* value $> 1 \times 10^{-6}$ and a number of beads <3 were set to missing. Samples with missing data in >5% of CpGs were excluded, as well as CpGs with missing data in >5% of samples. Samples identified with outlier values in bisulfite intensity, total intensity or beta-value distribution according to the ENmix quality control function were also excluded. Polymorphic (probes containing single nucleotide polymorphisms at the interrogated CpG site) and cross-hybridising probes (probes mapping to multiple regions of the genome) were filtered using the DMRcate package (Peters *et al.*, 2015). Out of the 63 MGC samples, 59 remained for analysis. All 118 leukocyte samples passed quality control filters. These methylation beta-values were used for the analysis of DNAm aberrations.

Epigenetic ageing analysis

The online DNA Methylation Age Calculator (https://dnamage. genetics.ucla.edu/home) was used to estimate DNAm age. As recommended by the authors, noob normalization was performed in minfi (Aryee et al., 2014) to obtain beta-values. The MGCs and leukocytes were analysed separately. Age acceleration difference was defined as the difference between DNAm age and chronological age, while age acceleration residuals as the residuals of DNAm age regressed on chronological age. An improved DNAm age predictor for MGCs (Granulosa Cell clock) was developed by adding 27 MGC samples with normal AMH levels to a subset ($n = 621$) of the samples used to train the Skin & Blood clock (Horvath et al., 2018; Levine et al., 2018). Only studies with publicly available intensity data (∗.IDAT) files were included in the training set of this predictor (GSE104471, GSE109042, GSE111223, GSE77136 and GSE80261). The Granulosa Cell clock was built following the methods described in the development of the Skin & Blood clock (Horvath et al., 2018; Levine et al., 2018). Briefly, a transformed version of chronological age, which has a logarithmic dependence until the age of 20 and linear dependence afterwards, was regressed on 452 567 CpG sites shared between the Illumina 450 K and EPIC methylation arrays using an elastic regression model (10-fold cross validation to select lambda) that automatically selected 296 CpG sites. The predictor was tested on the remaining 32 MGC samples and the 118 leukocytes samples, which were not part of the training set.

Predicted telomere length analysis

Similar to the estimation of DNAm age the online DNA Methylation Age Calculator (https://dnamage.genetics.ucla.edu/home) was used to estimate DNAmTL. The predictor outputs a measure of leukocyte telomere length, in which higher numbers indicate longer telomeres (Lu et al., 2019).

Accumulation of DNAm aberrations

DNAm aberrations, potential epimutations, were defined as outliers across all samples of the same tissue type (Gentilini et al., 2015). These outliers were defined as values greater than or less than three times the interquartile range from the upper or lower quartiles, respectively.

DMR analysis

Differentially\ignorespacesmethylated\ignorespacesregions (DMR) analysis was performed using the DMRcate package (Peters et al., 2015) in R. Beta-values were converted to M-values, and missing data were imputed to the mean across all samples of the same tissue type. False discovery rate (FDR) was set at 10%. Gene ontology (GO) analysis was performed in R using the missMethyl package (Phipson et al., 2015) which accounts for the different number of probes per gene in the array.

Statistics

Differences between age groups were tested with one-way ANOVA. The number of epimutations in leukocytes and MGCs were compared with Wilcoxon test. The age-DMR analysis was conducted with DMRcate (Peters et al., 2015). Enrichments were tested using Fisher's exact test. The accuracy of the different epigenetic clocks was measured by estimating Pearson's correlation coefficient, the median error defined as the median absolute difference between DNAm age and chronological age. All statistical analyses were performed in R and the value of $P < 0.05$ was considered statistically significant. The age of the women used in analysis referred to the time of the oocyte retrieval.

Ethics

All human materials were donated under approval from The Scientific Ethical Committee of the Capital Region, Denmark (ethical approval number: H-16027088) and the Danish Data Protection Agency (ID-nr.: HGH-2016_086) and conducted in accordance with the Helsinki Declaration II. All participants gave informed consent before the inclusion in the study.

Results

Participant characteristics

A total of 119 women were included in the study. Buffy coats were collected from each participant and 63 contributed additionally with donation of their MGCs. Of note: one woman only participated with donation of her MGCs. An overview of our participant population is presented in Table I (all) and Supplementary Table SI (women donating MGCs). Chronological age at the time of oocyte retrieval ranged from 25–44 years (average = 33.9 years). Based on the women's AMH level and the age-expected AMH level described by Lee and coworkers (Lee et al., 2012), the participants were categorized into ovarian reserve groups: diminished ovarian reserve (DOR) (under the 10th percentile), Normal (25th to 75th percentile) and High (above the 90th percentile). Women over 40 years were not categorized from their AMH level because it is well established that most of these women experience a DOR (Klein and Sauer, 2001; Liu et al., 2011).

Prediction of the DNAm age

DNAm age was analysed with the multi-tissue age predictor developed by Steve Horvath (Horvath, 2013). A significant correlation between the DNAm age and the chronological age in leukocytes was confirmed (Pearson's correlation coefficient (cor) = 0.79; $P = 2.2 \times 10^{-26}$) (Supplementary Fig. S1A). The predicted mean age was 35.0 years compared with an average chronological age of 33.9. In contrast, no significant correlation was present between DNAm age and chronological age in the MGCs (cor = 0.16, $P = 0.21$). The DNAm age of MGCs was substantially lower than the chronological age of the women with an average age of 6.8 years (Supplementary Fig. S1). To further explore DNAm age, we applied an alternative age estimator: the Skin & Blood clock (Horvath et al., 2018; Levine et al., 2018), in which cells with the same primary origin as MGCs are well represented. The age predicted by the 391 CpG sites that comprise this clock was consistent with the women's chronological age in leukocytes (average = 33.0 years; cor = 0.92; $P = 4.0 \times 10^{-48}$), but the DNAm age was still substantially younger in the MGCs (Fig. 1A), with an average age of 2.7 years. However, using the Skin & Blood clock a minor correlation with age in MGCs was found (cor = 0.30; $P = 0.02$) (Fig. 1A); in addition, there was a weak correlation between MGCs and leukocytes (cor = 0.23; $P = 0.086$; Fig. 1B). The predicted DNAm age was younger whether

Table I Demographic and clinical characteristics of the participant population divided into four age groups.

	Age groups					
	Demographic & clinical characteristics					
	25–29 years	30–34 years	35–39 years	40–44 years	Overall	One-way ANOVA P value
Number [MGC[1]]	27 [20]	35 [19]	47 [18]	10 [6]	119 [63]	-
Age at oocyte retrieval	27.5 ± 1.2	32.1 ± 1.4	37.3 ± 1.5	41.7 ± 1.4	33.9 ± 4.7	2.2×10^{-16}
BMI (kg/m^2)	24.3 ± 4.2	24.5 ± 4.1	24.1 ± 3.5	24.2 ± 2.5	24.3 ± 3.8	0.977
AMH[2] (pmol/L)	27.5 ± 20.1 (2.2–86)	30.6 ± 22.3 (0.6–94)	18.8 ± 19.1 (0.2–68)	10.3 ± 16.2 (0.3–55)	23.5 ± 20.9 (0.2–94)	0.008
Ovarian reserve category						
- DOR[3]	5	5	13	-	23	-
- Normal	17	20	22	-	59	-
- High	5	10	12	-	27	-
- 40–44 years	-	-	-	10	10	-
Primary cause of infertility						
- Male factor	9	13	12	-	34	-
- Female factor	6	9	3	10	28	-
- Unexplained	12	11	16	-	39	-
- Other causes*	-	2	16	-	18	-
FSH (IU/L)	6.4 ± 2.4	5.7 ± 3.9	10.0 ± 8.8	8.0 ± 2.4	7.8 ± 6.4	0.017
LH (IU/L)	5.7 ± 4.7	5.5 ± 3.1	8.9 ± 9.5	6.5 ± 2.0	7.1 ± 6.9	0.195
LH/FSH ratio	1.1 ± 1.1	1.2 ± 0.6	1.0 ± 0.8	0.9 ± 0.5	1.04 ± 0.8	0.639
Prolactin (IU/L)	263 ± 135	325 ± 125	303 ± 142	236 ± 122	295 ± 135	0.195
TSH[4] (IU/L)**	1.5 ± 0.6	1.8 ± 0.8	1.8 ± 0.9	1.5 ± 0.5	1.7 ± 0.8	0.340
	Cycle characteristics					
No. of oocytes	9.7 ± 3.8	10.0 ± 6.5	6.3 ± 4.3	6.8 ± 5.3	8.1 ± 5.3	0.004
No. of 2PN[5] zygotes	5.7 ± 2.9	5.4 ± 4.2	3.1 ± 2.8	3.7 ± 4.1	4.4 ± 3.6	0.006
No. of clinically usable embryos	3.8 ± 2.5	3.2 ± 2.8	1.3 ± 1.8	2 ± 1.4	2.5 ± 2.4	5.9×10^{-05}
Utilization rate***	0.7 ± 0.3	0.6 ± 0.3	0.5 ± 0.4	0.7 ± 0.3	0.6 ± 0.3	0.027

Mean ± standard deviation (range).

*Single women and women with a female partner.

**This is baseline measurement. In case of TSH > 2.5 IU/L with +/− thyreoidea peroxidase (TPO) antibodies, regulation to <2.5 IU/L or 2.5–4.0 without TPO antibodies was ensured before treatment start following the Danish Fertility Society's Guideline.

***No. of clinically useable embryos/no. of 2PN zygotes.

[1] Mural granulosa cells

[2] Anti-Müllerian hormone

[3] Diminished ovarian reserve

[4] Thyroid-stimulating\ignorespaceshormone

[5] Two pronuclear

the MGCs were derived from women with low ovarian reserve (women with DOR or age > 40 years) or from women with normal or high ovarian reserve (Fig. 1A). Adjusting for AMH levels or the ovarian stimulation regimens did not change the age acceleration.

We then looked at the association between age acceleration difference and chronological age (Fig. 1C and D). The age acceleration difference was small in leukocytes (median = −1.04; range = −6.32 to 4.77) and showed a positive correlation with chronological age (cor = 0.41; P = 0.001); in contrast, in MGCs the difference was large in absolute values (median = −29.96; range = −41.54 to −22.99), was negative and increased in magnitude with age (cor = −0.99; $P = 2.4 \times 10^{-47}$; Fig. 1C). As expected from the latter observation, we found a negative correlation (cor = −0.42, P = 0.001) in the age acceleration differences between leukocytes and MGCs (Fig. 1D).
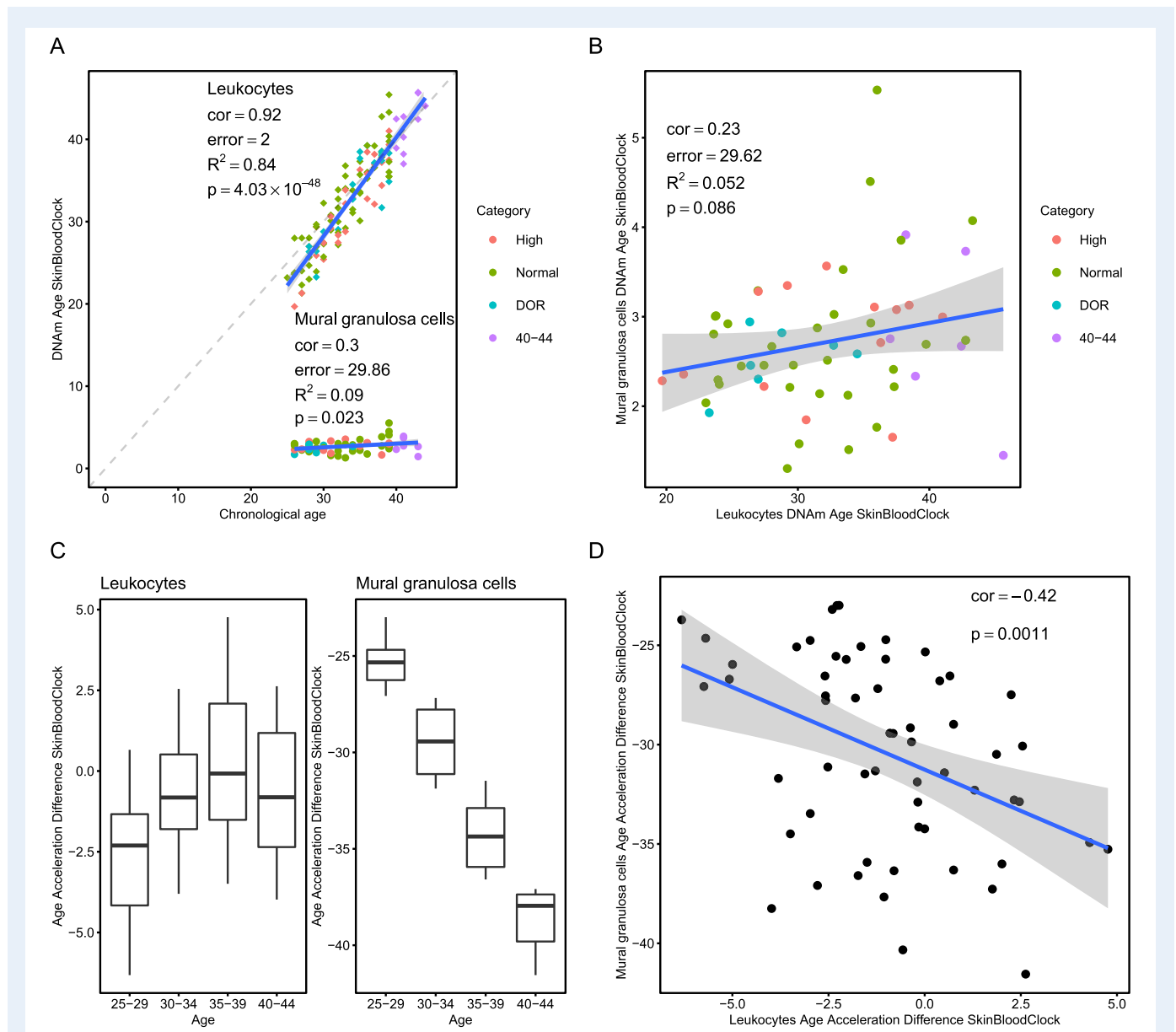
Figure 1 Epigenetic age in mural granulosa cells and leukocytes. (**A**) DNAm age in granulosa cells ($n = 59$) and leukocytes ($n = 118$) using Horvath's Skin & Blood clock. Dashed line indicates a perfect prediction ($y = x$). The participants are divided into groups regarding their ovarian reserve status, indicated with colours: blue = diminished ovarian reserve (DOR), green = Normal, red = High, purple = 40–44 years. (**B**) Scatter plot illustrating the correlation between the DNAm age of leukocytes and granulosa cells collected from the same individual. (**C**) Box plots of the age acceleration differences in the two cell types. The women are divided into age groups (25–29, 30–34, 35–39 and 40–44 years). The age acceleration difference magnitudes are greatest in the oldest age group in the granulosa cells (max(absolute values) = 41.55). The leukocytes exhibit a different pattern with only a slight age acceleration difference (max(absolute values) = 6.32). (**D**) Scatter plot showing the association of age acceleration differences between the two cell types (correlation (cor) = −0.42, $P = 0.001$).

A granulosa cell clock

Due to the poor correlation in DNAm and chronological age for MGCs, we decided to improve the Skin & Blood epigenetic age estimator by incorporating 27 of our MGC samples in a training set (which we name the Granulosa Cell clock). The Granulosa Cell clock we developed consists of 296 CpG sites (Supplementary Table SII). Figure 2A shows the prediction of DNAm age of the remaining 32 MGC samples that were not used in the training set; the Granulosa Cell clock yielded an improved correlation of

0.47 ($P = 0.006$). When applying the Granulosa Cell clock to our leukocyte data a good correlation was found (cor = 0.85, $P = 4.3 \times 10^{-34}$). Supplementary Figure S2A shows the intersection between the Skin & Blood clock and the Granulosa Cells clock (37 CpGs). The genomic distribution of the clock type specific CpG sites—354 CpGs in the Skin & Blood clock, and 259 CpGs in the Granulosa Cell clock—is shown in Supplementary Fig. S2B. When comparing the mean DNAm levels of each CpG across all samples
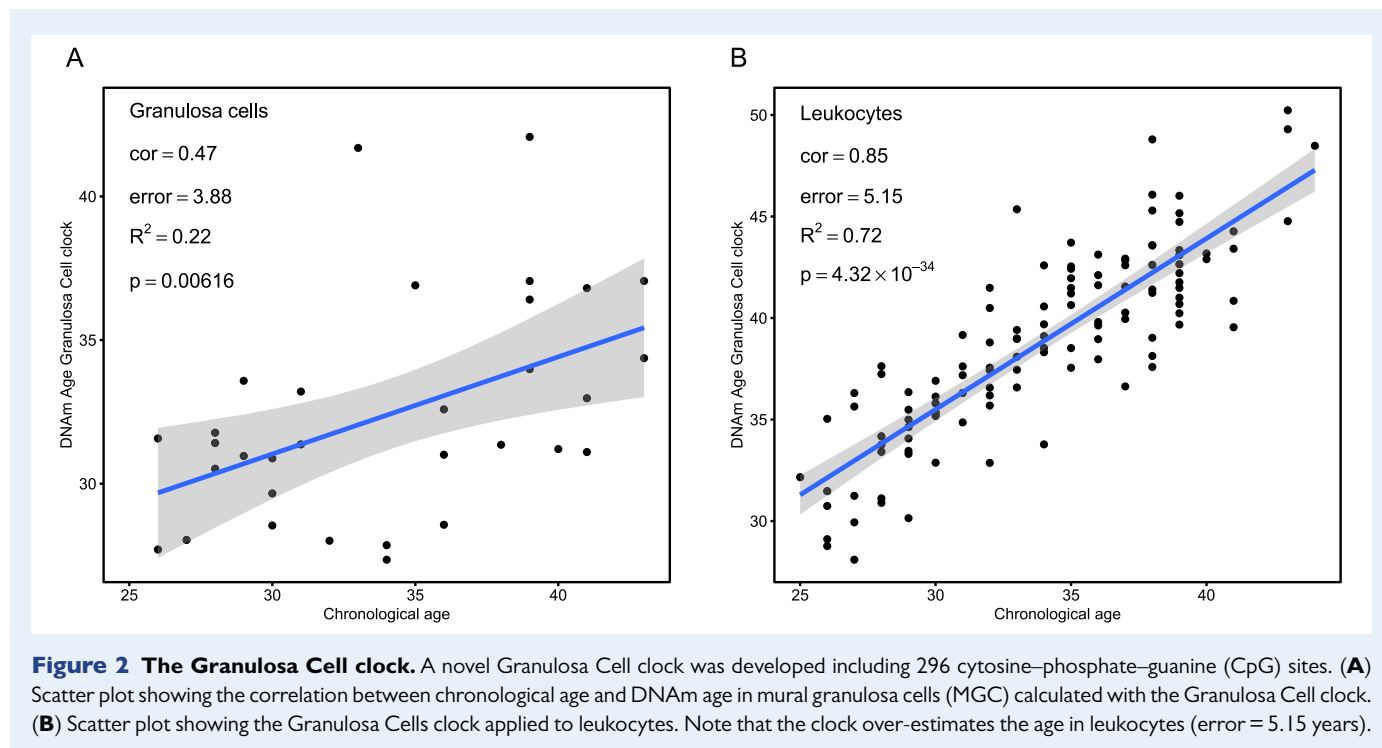
Figure 2 The Granulosa Cell clock. A novel Granulosa Cell clock was developed including 296 cytosine–phosphate–guanine (CpG) sites. (**A**) Scatter plot showing the correlation between chronological age and DNAm age in mural granulosa cells (MGC) calculated with the Granulosa Cell clock. (**B**) Scatter plot showing the Granulosa Cells clock applied to leukocytes. Note that the clock over-estimates the age in leukocytes (error = 5.15 years).

between leukocytes and MGCs, it is evident that the DNAm levels of the CpG sites in the Granulosa Cell clock are shared between the two tissues, whereas those in the Skin & Blood clock are not (Supplementary Fig. S2C).

Predicted telomere length

Telomere length is another biomarker of ageing that can be predicted from DNAm profiles.

DNAmTL was calculated for both cell types. In leukocytes, telomere length was negatively correlated with age (cor = -0.62, $P = 4.0 \times 10^{-14}$) (Fig. 3A), while in MGC telomere length was shorter and unaffected by age (cor = -0.1, $P = 0.47$) (Fig. 3B).

Epimutations

As another measure of ageing we used the accumulation of errors in DNAm (here defined as epimutations). We observed that epimutations increased exponentially with advanced maternal age in both tissues. However, the rate of increase was higher in MGCs (Fig. 4A). Overall, epimutations were more frequent in MGCs (paired samples Wilcoxon test; $P = 0.003$) compared with leukocytes of the same women (Fig. 4B). We found no association between the total dose of FSH and the number of epimutations (leukocytes: cor = 0.14, $P = 0.54$, MGCs: cor = 0.32, $P = 0.053$). Epimutated sites showed a moderate enrichment in intergenic regions (odds ratio (OR) = 1.18; $P = 1.1 \times 10^{-171}$) and depletion close to promoter regions (0–200 base pair (bp) upstream of the transcription start site) (OR = 0.71; $P = 1.4 \times 10^{-264}$).

Epigenome-wide association study

To further study the relationship between ageing and DNAm we conducted an epigenome-wide association study (EWAS) of chronological age. Due to limited sample size, we were underpowered to detect genome-wide significant signals ($P < 5 \times 10^{-8}$) at single CpG site resolution (power = 0.00, effect size = 0.15) (Supplementary Fig. S3). In order to increase the statistical power to detect differences, we conducted the identification of DMRs in the extremes of our sample (women under 30 years old ($n = 19$) and women above 40 ($n = 6$); only one woman with PCOS as her secondary diagnosis was in those age groups and included in this analysis, which however did not affect the result (data not shown)). A total of 335 DMRs associated with age (age-DMRs) were identified in MGCs and only one in leukocytes (Supplementary Table SIII). The most significant signal in MGCs was identified at the metastable-epiallele vault RNA 2-1 (*VTRNA2-1*), where a gain of methylation was observed that was significant in MGCs but not leukocytes (Fig. 5 and Supplementary Fig. S4). The second most significant signal was found in the *AMH* gene where a gain of methylation in the gene body was observed in MGCs (Supplementary Table SIII, full list; Table II, selected genes). Out of the 335 age-DMRs, 311 showed a loss of methylation with age, while only 24 gained methylation. Age-DMRs were enriched in promoters (0–200 bp upstream of the transcription start site) (Fisher's exact test; OR = 3.32; $P = 7.1 \times 10^{-122}$). GO analysis of the genes associated with the 335 age-DMRs revealed an enrichment for ribonucleic acid (RNA) processing ($P = 3.96 \times 10^{-08}$) and gene expression ($P = 2.3 \times 10^{-06}$) (Supplementary Table SIV). In addition, we tested for enrichment in gene lists related to reproduction and granulosa cell expression profiles (Supplementary Table SV). We tested for enrichment in genes involved in female reproductive system disease and infertility (https://gemma.msl.ubc.ca/phenotypes.html) (Zoubarev *et al.*, 2012), genes expressed in granulosa cells after ovulation induction (Grøndahl *et al.*, 2012) and genes expressed in granulosa cells prior to hCG (Wissing *et al.*, 2014). Only genes involved in Female Reproductive System Disease showed an
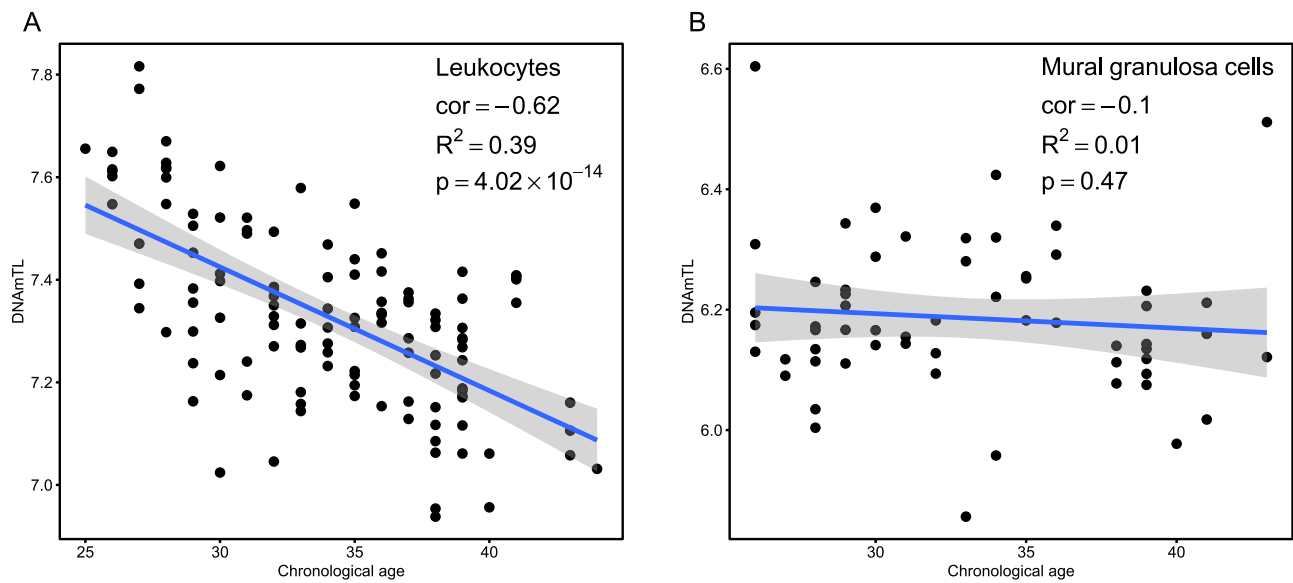
Figure 3 Predicted telomere length in mural granulosa cells and leukocytes. The predicted telomere length (DNAmTL) in relation to age. Scatter plots indicating the Pearson's correlation coefficient (cor) between predicted telomere length and age in leukocytes (**A**) and MGC (**B**).
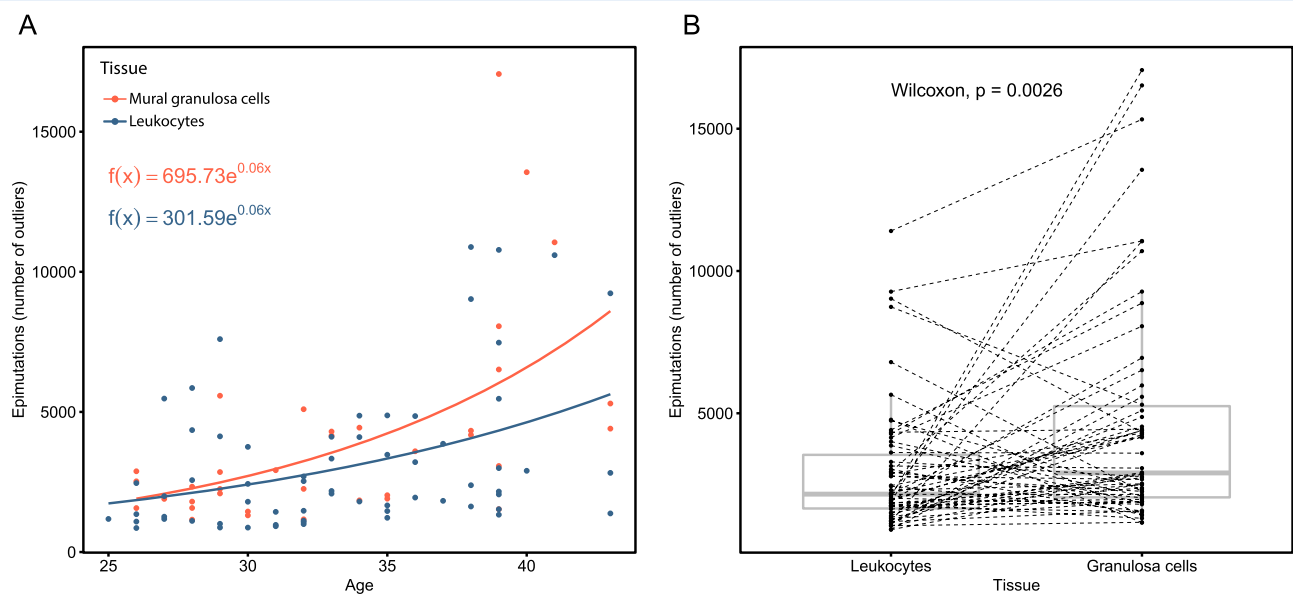

Figure 4 Epimutations in mural granulosa cells and leukocytes. Epimutations (number of outliers) in relation to age. (**A**) Scatter plot indicated the number of epimutations as a function of age in MGC (red) and leukocytes (blue), with exponential lines of best fit. (**B**) Comparison of epimutations in paired MGC and leukocyte samples; boxes represent the interquartile range, with the media values depicted by the horizontal bar; Wilcoxon test, $P = 0.003$ (mean of differences = 1693.5).

over-representation ($P = 0.006$). As a negative control to ensure we were not observing a spurious signal, we also tested a random gene list with a similar number of genes (disease by infectious disease), which showed no significant enrichment ($P = 0.16$).

Discussion

Our data clearly demonstrate that MGCs from the human ovary have a distinctive epigenetic ageing profile compared with blood collected

from the same woman. To our knowledge, these data show that MGCs have the largest error predicated by the multi-tissue DNAm clock. As expected, we found a significant correlation between DNAm age and chronological age in leukocytes with both the multi-tissue age predictor (Horvath, 2013) and the Skin & Blood clock (Horvath *et al.*, 2018). The MGC, on the other hand, showed no or limited correlation with chronological age, which, together with their substantially younger DNAm age, suggests that MGC age epigenetically differently and

Table II Age-DMRs of selected genes.

Gene name	Gene symbol	Chromosome	DMR[6] width	No. of CpGs[7]	Min. FDR[8]	Stouffer	Mean beta fold change
Vault RNA 2-1	VTRNA2-1	5	1756	17	3.4×10^{-34}	3.6×10^{-6}	0.1832
Anti-Müllerian hormone	AMH	19	2954	16	3.8×10^{-19}	4.1×10^{-5}	−0.0994
Zinc finger protein 57	ZFP57	6	924	21	2.5×10^{-25}	4.5×10^{-4}	−0.1794
Glyceraldehyde-3-phosphate dehydrogenase	GAPDH	12	285	2	2.6×10^{-15}	0.0104	−0.0791
Aquaporin 2	AQP2	12	771	10	6.4×10^{-21}	0.0121	−0.0662
Growth hormone receptor	GHR	5	108	2	1.6×10^{-7}	0.0390	−0.0556
Placental growth factor	PGF	14	304	6	7.8×10^{-8}	0.1999	−0.0084
Cytochrome P450 family 26 subfamily A member 1	CYP26A1	10	173	6	1.1×10^{-7}	0.2170	−0.0156
Estrogen receptor 1	ESR1	6	44	2	2.5×10^{-7}	0.3760	−0.0501
Growth hormone secretagogue receptor	GHSR	3	336	9	1.4×10^{-7}	0.7644	−0.0145

[6] Differentially methylated regions
[7] Cytosine–phosphate–guanine
[8] False discovery rate

independently from other somatic cells in the body. Not surprisingly, these results are consistent with findings in cumulus cells, which showed an average DNAm age, based on the multi-tissue age predictor, of 9.3 years regardless of the chronological age of the women (comparison of two age groups; young (32.8 years) vs. old (41.9 years)) (Morin *et al.*, 2018). We conclude that ageing of the somatic cells in the ovary affects different DNAm sites than the sites found in other tissue types. Although the association was limited, our results indicate that women with a young DNAm age of their leukocytes also have a younger DNAm age in their MGC. We further demonstrated that the magnitude of the age acceleration differences of the MGC gradually elevated with advanced age. This may partially be explained by the limited correlation with chronological age and the reduced range in the DNAm age estimates.

The multi-tissue age predictor did not perform well in the MGC, which could be explained by the lack of MGC in the training data set during the development of the multi-tissue age predictor. However, the predictor has previously been shown to provide accurate estimates of chronological age for tissues not represented in the training data (e.g. oesophagus, jejunum, pancreas, spleen) (Horvath, 2013). Intriguingly, the Skin & Blood clock also lacks MGC in its training set but was able to show at least a weak correlation with chronological age. A plausible explanation could be that the tissues used to train this clock were closer in origin to MGC. The Skin & Blood clock was designed having in mind its performance in fibroblasts and other cell types/tissues used in *ex vivo* studies, such as keratinocytes, buccal cells, endothelial cells, lymphoblastoid cells, skin, blood and saliva. Cells of mesodermal origin, as MGC are (Sawyer *et al.*, 2002), are well represented in this clock. By improving the Skin & Blood clock with the development of the Granulosa Cell clock we were able to detect a correlation between DNAm age and chronological age in MGC. However, the DNAm age was somewhat over-estimated when applying the Granulosa Cell clock to our leukocyte data, which again suggests that MGC are epigenetically different from other somatic cells. The Granulosa Cell

clock could be capturing a fraction of mitotic ageing, which explains why leukocytes with a history of more cell divisions show a higher DNAm age. In addition, the genomic distribution of the CpG content of the two clocks differs, primarily in the proportion of CpGs in islands (28 vs. 38%) and open sea, defined as isolated CpGs located >4 kb from a CpG island, (38 vs. 26%). Even though the Skin & Blood clock and the Granulosa Cell clock only have 37 CpG sites in common, the Granulosa cell clock performed well in both cell types, suggesting that the 354 CpG sites included in the Skin & Blood clock are not exclusive to the ageing process of somatic cells. We observed an enrichment in CpG islands in the intersected CpG sites compared with background (all sites in the array). From studies in other tissues, it is known that gains of methylation at CpG island promoters are observed in age-DMRs (Rakyan *et al.*, 2010; Teschendorff *et al.*, 2010; Bell *et al.*, 2016). Methylation acquisition with age at promoters of genes, such as the well replicated fatty acid elongase 2 gene (*ELOVL2*) (Sawyer *et al.*, 2002), might be shared across all cell types, and that is why we observe this enrichment at the intersected CpG sites.

To further explore the ageing process, we calculated the DNAmTL. Shorter telomere length has been shown to correlate with advanced age in other cell types (Shammas, 2011). The expected correlation between chronological age and DNAmTL was found in the leukocytes; however, we found that the DNAmTL of MGC was shorter and unaffected by age, which may reflect that the DNAmTL predictor was trained in blood and fails to predict the telomere length in MGC. Interestingly, Morin *et al.*, found the opposite in cumulus cells, where cumulus cells have a longer relative telomere length than white blood cells from women pursuing ART treatment (Morin *et al.*, 2018). However, the study had actual measures and not estimates from DNAm profiles. Granulosa cells proliferate rapidly throughout the late phase of folliculogenesis (from 30 pre-granulosa cells in the primordial follicle (Westergaard *et al.*, 2007) to around 60 million in the ovulatory follicle (Hirshfield, 1985; Gougeon, 1996)). It has been suggested that granulosa cells have shorter telomere length, despite the
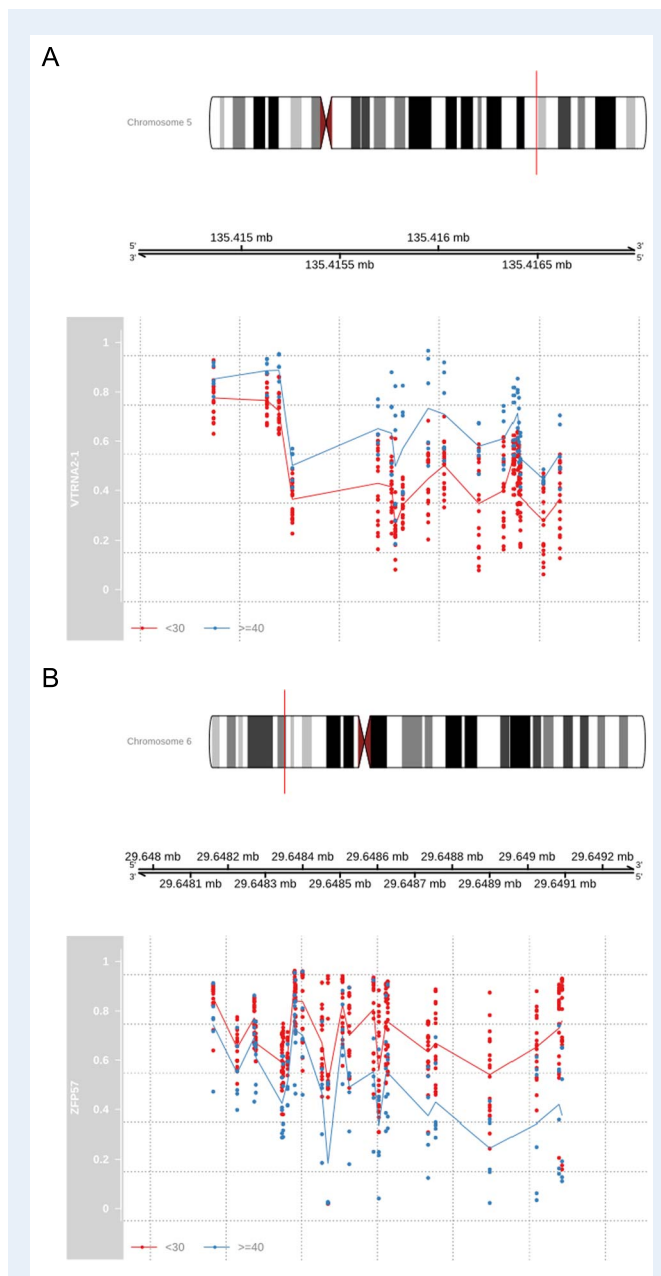
Figure 5 Epialleles in mural granulosa cells from women < 30 years and ≥ 40 years of age. (**A**) EWAS of chronological age in MGC, illustrated by the most significant signal (Stouffer = 3.62×10^{-6}) detected at the meta-stable epiallele VTRNA2-1 in chromosome 5. Methylation at CpGs within VTRNA2-1 comparing values in young (<30 years; red) and older women (≥40 years; blue); mean beta fold change = 0.18. (**B**) Another significant signal (Stouffer = 4.5×10^{-4}) also located in a putative meta-stable epiallele was observed in ZFP57 on chromosome 6, where women under 30 years showed on average greater methylation levels (mean beta fold change = −0.18). The unit of the chromosome length measurements are mega base (mb).

presence of active telomerase, which functions to restore shortened telomeres (Kosebent et al., 2018). The microenvironment of granulosa cells contains oestrogens reported to influence telomerase activity (Bayne et al., 2011) as well as other agents with potential influence on

telomere length (Kosebent et al., 2018). Since MGC are unique cells in terms of their many years or decades of quiescence followed by an accelerated mitotic activity, they may represent another aspect of ageing than other cells. We already know that compromised repair of DNA double strand breaks is associated with accelerated loss of ovarian follicles and accumulation of double strand breaks in human oocytes (Titus et al., 2013) and that the capacity of pre-granulosa cells to repair double-strand breaks declines with increasing age (Zhang et al., 2015) in non-human primates, suggesting that also the MGCs are affected by advanced age.

DNAm age and predicted telomere length can be used as a prediction of chronological age or as a reflection of biological ageing; however, they are not a measure of the actual ageing process and might reflect different aspects of ageing. Therefore, as a third approach to study ageing in MGCs, we investigated the frequency of epimutations, which are not restricted only to a limited subset of CpGs in the array. The notion that epimutations accumulate during the lifetime first gained prominence from the epigenetic divergence observed in identical twins; during early life, twins were indistinguishable at sites assayed for DNAm, but became divergent at older ages (Fraga et al., 2005). More recent studies examining methylation in peripheral blood from infants to centenarians have reported an exponential increase in epimutations with age (Gentilini et al., 2015). We also observed that the number of epimutations in MGC increases substantially with advancing age. We found a significantly higher frequency of epimutations in intergenic regions of the genome, which makes us speculate that promotor regions, which are often more conserved, are partially more protected from these types of events. However, the number of epimutations was significantly greater in MGC compared to leukocytes. This may due to hormonal exposure of these cells during COS and investigating epimutations in MGC from a natural cycle would remove the potential confound of COS. However, women treated with high dose of FSH did not have a higher number of epimutations compared with women treated with a low dose of FSH, suggesting that the relatively short time of hormone exposure does not influence the epigenetics in mature follicles. Still, it remains unknown when during folliculogenesis the epimutations occur.

Finally, EWAS data revealed 335 DMRs when comparing MGC from young (<30 years) and reproductively older women (≥40 years). These age-DMRs were not observed in leukocytes from the same participants or generally reported in other tissues (Day et al., 2013), suggesting a different ageing process in MGC. Interestingly, the comparison in leukocytes identified only one age-DMR, which may suggest that more drastic changes with age occur in MGC as a potential reflection of the loss of function in the ovarian follicle (the competence of the oocyte) with increasing age. The age-DMR found in the leukocytes was in the *REC8* meiotic recombination protein gene, which encodes the REC8 protein involved in the meiotic cohesin complex that binds sister chromatids (Parisi et al., 1999). Decreased level of REC8 in dictyate-stage oocytes (before resumption of meiosis) in women ≥40 years has been suggested to partly explain the high frequency of aneuploidy found in oocytes from women with advanced maternal age (Tsutsumi et al., 2014). Interestingly, *REC8* has been added to the list of candidate genes for premature ovarian insufficiency (POI), as a mutation was found in blood from two women diagnosed with POI (Bouilly et al., 2016).

Furthermore, changes in the DNAm of *REC8* in leukocytes were recently suggested to be a biomarker for cancer risk (Bartlett *et al.*, 2019). Whether *REC8* DNAm in leucocytes relates to female fertility and general health is unclear and needs further exploration before drawing any conclusions.

The most significant signal we identified in MGC was at the *VTRNA2-1* epiallele, which exhibited a gain of methylation. Even though this is a metastable epiallele with a methylation level that varies between individuals but generally considered to be shared across tissues from the same individual (Silver *et al.*, 2015), we only observed this signal in MGC and not in leukocytes, again suggesting that MGC differ from other somatic cell types. Another significant signal observed was increased methylation in the zinc finger protein 57 homolog (*ZFP57)* gene, which is a significant factor in DNAm maintenance and has been linked with metastable epiallele methylation (Kessler *et al.*, 2018). The possible functional significance of this finding is unclear at this stage; recently, ovarian dysfunction after prenatal exposure to insecticide has been connected to altered expression of downstream *ZFP57* target genes in the adult mouse ovary (Legoff *et al.*, 2019).

GO analysis of the MGC age-DMRs revealed enrichment in pathways related to gene transcription. Studies in other somatic cells have suggested a global deregulation of gene expression with age and also a decrease in the amount of processed messenger RNA (mRNA) in aged cells (Sawyer *et al.*, 2002). Our results suggest that MGCs are not the exception and might be experiencing a similar effect on mRNA processing at a relatively early age. Interestingly, the second most significant signal we found was in the *AMH* gene, with increased methylation in the gene body. AMH is produced by the granulosa cells of small growing follicles and plays a key role in folliculogenesis (Rajpert-De Meyts *et al.*, 1999). The expression of AMH (both mRNA and protein) in human granulosa cells wanes with increasing size of the human follicle (Grøndahl *et al.*, 2011; Kristensen *et al.*, 2017) reaching a stable low level in MGC isolated from pre-ovulatory follicles before ovulation induction and at oocyte retrieval (Wissing *et al.*, 2014). The primary factors regulating AMH expression in granulosa cells are oocyte derived factors: growth differentiation factor 9 (GDF9) and bone morphogenetic protein 15 (BMP15), as well as FSH (Roy *et al.*, 2018). As methylation of gene bodies primarily has been correlated with increased expression (Jjingo *et al.*, 2012), our finding suggests an age-related higher expression of AMH in the pre-ovulatory follicle, which may reflect an altered communication between the oocyte and granulosa cells. These findings are supported by Yu *et al.*,, who found age-related changes in the *AMH* gene in human granulosa cells (Yu *et al.*, 2015). It had been shown that the concentration of GDF9 in the follicular fluid decreases with increasing age of women, indicating an alteration in the secretion of oocyte specific factors with age (Han *et al.*, 2011). Other genes associated with age-DMRs in MGC were placenta growth factor (*PGF*), growth hormone secretagogue receptor (*GHSR*) and growth hormone receptor (*GHR*); all reported to be involved in folliculogenesis. PGF is expressed by MGC and is required for ovulation, luteinization and follicular angiogenesis in primates (Bender *et al.*, 2018), and GHSR in mice has been shown to be activated in response to stress resulting in a reduced number of primordial follicles (Natale *et al.*, 2019). Furthermore, a recent study showed a lower number of GHR in MGC in reproductive older women compared with younger women (Regan *et al.*, 2018). Our findings thus support and extend an association between age and these genes in the ovarian follicle. However, whether the changes are causative (as expected for promotor methylation) or a consequence (as in gene-body methylation) of changes in gene expression is unknown and needs further investigation. Due to a limited number of cells from the MGC collection, we were not able to perform a gene expression analysis to evaluate whether the epigenetic findings are correlated with changes in the gene expression in the MGC.

With the comparison of two somatic cell types, our findings suggest that MGCs age differently to non-ovarian somatic cells in the human body. MGCs play a pivotal role in folliculogenesis and in the interaction with the oocyte, so further knowledge about ageing of the MGC might give us important insights into ageing of the oocyte itself. How can we reconcile the seemingly discordant effects we observe in MGC in DNAm age prediction, estimated telomere length and age-related increase in epimutations? One possibility is that these outcomes are associated with different aspects of ageing and the unique biology of MGCs and the ovarian follicle. For instance, MGCs may experience a similar, fixed process of proliferation and expansion once the follicle is activated irrespective of when during the woman's life course it occurs. In contrast, with increasing age, the length of time that the follicle has remained in the dormant state increases. Therefore, if telomere length and predicted DNAm age are properties very much associated with mitotic events, these parameters will be similar whatever the chronological age of the donor. The increase in epimutations we observe with age in MGCs might therefore indicate that these DNAm aberrations are accumulating mostly in the period of extended follicle dormancy. One potential consequence is that the epigenetic fidelity of ovarian somatic cells at the time of follicular recruitment in older women is impaired.

More studies are needed to establish whether our Granulosa Cell clock or epimutation detection could be used to detect premature reproductive ageing in women and to investigate whether the clock is also applicable to cumulus cell or other cells of the human ovary.

Although invasive, this knowledge could potentially give us a tool to determine an individual's pace of reproductive ageing, thereby giving women a better chance to plan the best time for pregnancy.

Supplementary data

Supplementary data are available at *Human Reproduction* online.

Acknowledgements

We thank all participating women for their willingness to participate in the study. We also want to express our gratitude to all nurses and embryologists, who were involved in the patient recruitment and material sampling at Herlev Hospital, Hvidovre Hospital, Skåne University Hospital and Stork IVF Clinic A/S.

Authors' roles

K.W.O., M.L.G. and R.B. designed and initiated the study. K.W.O., A.Z., N.l.C.F. and M.B. were involved in patient recruitment and sample collection. K.W.O., J.C.F., M.L.G. and G.K. were involved in the analysis and interpretation of data and participated in writing and finalising the manuscript. J.C.F. and A.C. performed the bioinformatic analysis and

References

Aryee MJ, Jaffe AE, Corrada-Bravo H, Ladd-Acosta C, Feinberg AP, Hansen KD, Irizarry RA. Minfi: a flexible and comprehensive bioconductor package for the analysis of Infinium DNA methylation microarrays. *Bioinformatics* 2014;**10**:1363–1369.

Baird DT, Collins J, Egozcue J, Evers LH, Gianaroli L, Leridon H, Sunde A, Templeton A, Van Steirteghem A, Cohen J *et al*. Fertility and ageing. *Hum Reprod Update* 2005;**3**:261–276.

Bartlett AH, Liang JW, Sandoval-Sierra JV, Fowke JH, Simonsick EM, Johnson KC, Mozhui K. Longitudinal study of leukocyte DNA methylation and biomarkers for cancer risk in older adults. *Biomark Res* 2019;**10**:1–13.

Bayne S, Li H, Jones ME, Pinto AR, van Sinderen M, Drummond A, Simpson ER, Liu JP. Estrogen deficiency reversibly induces telomere shortening in mouse granulosa cells and ovarian aging in vivo. *Protein Cell* 2011;**4**:333–346.

Bell CG, Xia Y, Yuan W, Gao F, Ward K, Roos L, Mangino M, Hysi PG, Bell J, Wang J *et al*. Novel regional age-associated DNA methylation changes within human common disease-associated loci. *Genome Biol* 2016;**1**:193.

Bender HR, Trau HA, Duffy DM. Placental growth factor is required for ovulation, luteinization, and angiogenesis in primate ovulatory follicles. *Endocrinology* 2018;**2**:710–722.

Bergstrom CT, Pritchard J. Germline bottlenecks and the evolutionary maintenance of mitochondrial genomes. *Genetics* 1998;**4**:2135–2146.

Binder AM, Corvalan C, Mericq V, Pereira A, Santos JL, Horvath S, Shepherd J, Michels KB. Faster ticking rate of the epigenetic clock is associated with faster pubertal development in girls. *Epigenetics* 2018;**1**:85–94.

Bouilly J, Beau I, Barraud S, Bernard V, Azibi K, Fagart J, Fèvre A, Todeschini AL, Veitia RA, Beldjord C *et al*. Identification of multiple gene mutations accounts for a new genetic architecture of primary ovarian insufficiency. *J Clin Endocrinol Metab* 2016;**12**:4541–4550.

Ceylan B, Ozerdogan N. Factors affecting age of onset of menopause and determination of quality of life in menopause. *Turk J Obstet Gynecol* 2015;**1**:43–49.

Day K, Waite LL, Thalacker-Mercer A, West A, Bamman MM, Brooks JD, Myers RM, Absher D. Differential DNA methylation with age displays both common and dynamic features across human tissues that are influenced by CpG landscape. *Genome Biol* 2013;**9**:1–19.

Dorrington JH, Moon YS, Armstrong DT. Estradiol-17beta biosynthesis in cultured granulosa cells from hypophysectomized immature rats; stimulation by follicle-stimulating hormone. *Endocrinology* 1975;**5**:1328–1331.

Eppig JJ. Oocyte control of ovarian follicular development and function in mammals. *Reproduction* 2001;**6**:829–838.

Fraga MF, Ballestar E, Paz MF, Ropero S, Setien F, Ballestar ML, Heine-Suner D, Cigudosa JC, Urioste M, Benitez J *et al*. Epigenetic differences arise during the lifetime of monozygotic twins. *Proc Natl Acad Sci U S A* 2005;**30**:10604–10609.

Franasiak JM, Forman EJ, Hong KH, Werner MD, Upham KM, Treff NR, Scott RT Jr. The nature of aneuploidy with increasing age of the female partner: a review of 15,169 consecutive trophectoderm biopsies evaluated with comprehensive chromosomal screening. *Fertil Steril* 2014;**3**:656–663.

Gentilini D, Garagnani P, Pisoni S, Bacalini MG, Calzari L, Mari D, Vitale G, Franceschi C, Di Blasio AM. Stochastic epigenetic mutations (DNA methylation) increase exponentially in human aging and correlate with X chromosome inactivation skewing in females. *Aging* 2015;**8**:568–578.

Gilchrist RB, Lane M, Thompson JG. Oocyte-secreted factors: regulators of cumulus cell function and oocyte quality. *Hum Reprod Update* 2008;**2**:159–177.

Giuliani C, Cilli E, Bacalini MG, Pirazzini C, Sazzini M, Gruppioni G, Franceschi C, Garagnani P, Luiselli D. Inferring chronological age from DNA methylation patterns of human teeth. *Am J Phys Anthropol* 2016;**4**:585–595.

Gougeon A. Regulation of ovarian follicular development in primates: facts and hypotheses. *Endocr Rev* 1996;**2**:121–155.

Grøndahl ML, Andersen CY, Bogstad J, Borgbo T, Boujida VH, Borup R. Specific genes are selectively expressed between cumulus and granulosa cells from individual human pre-ovulatory follicles. *Mol Hum Reprod* 2012;**12**:572–584.

Grøndahl ML, Nielsen ME, Dal Canto MB, Fadini R, Rasmussen IA, Westergaard LG, Kristensen SG, Yding AC. Anti-Mullerian hormone remains highly expressed in human cumulus cells during the final stages of folliculogenesis. *Reprod Biomed Online* 2011;**4**:389–398.

Han M, Park SB, Park BJ. Lower growth factor expression in follicular fluid undergone in-vitro fertilization. *Clin Exp Reprod Med* 2011;**4**:210–215.

Hirshfield A. Comparison of granulosa cell proliferation in small follicles of hypophysectomized, prepubertal, and mature rats. *Biol Reprod* 1985;**4**:979–987.

Horvath S. DNA methylation age of human tissues and cell types. *Genome Biol* 2013;**10**: R115.

Horvath S, Mah V, Lu AT, Woo JS, Choi OW, Jasinska AJ, Riancho JA, Tung S, Coles NS, Braun J *et al.* The cerebellum ages slowly according to the epigenetic clock. *Aging* 2015a;**5**:294–306.

Horvath S, Oshima J, Martin GM, Lu AT, Quach A, Cohen H, Felton S, Matsuyama M, Lowe D, Kabacik S *et al.* Epigenetic clock for skin and blood cells applied to Hutchinson Gilford Progeria syndrome and ex vivo studies. *Aging* 2018;**7**:1758–1775.

Horvath S, Pirazzini C, Bacalini MG, Gentilini D, Di Blasio AM, Delledonne M, Mari D, Arosio B, Monti D, Passarino G *et al.* Decreased epigenetic age of PBMCs from Italian semisupercentenarians and their offspring. *Aging* 2015b;**12**:1159–1170.

Illumina. Infinium® HD Assay Methylation Protocol Guide. 2015.

Jjingo D, Conley AB, Yi SV, Lunyak VV, Jordan IK. On the presence and role of human gene-body DNA methylation. *Oncotarget* 2012;**4**: 462–474.

Kessler N, Waterland R, Prentice A, Silver M. Establishment of environmentally sensitive DNA methylation states in the very early human embryo. *Sci Adv* 2018;**7**: eaat2624.

Klein J, Sauer MV. Assessing fertility in women of advanced reproductive age. *Am J Obstet Gynecol* 2001;**3**:758–770.

Kosebent EG, Uysal F, Ozturk S. Telomere length and telomerase activity during folliculogenesis in mammals. *J Reprod Dev* 2018;**6**: 477–484.

Kristensen SG, Mamsen LS, Jeppesen JV, Bøtkjær JA, Pors SE, Borgbo T, Ernst E, Macklon KT, Andersen CY. Hallmarks of human small antral follicle development: implications for regulation of ovarian steroidogenesis and selection of the dominant follicle. *Front Endocrinol (Lausanne)* 2017;**376**:1–10.

Lee JE, Park DS, Kim M-L, Yoon BS, Song T, Kim MK, Seong SJ, Kim Y-J. Age-related distribution of anti-Müllerian hormone levels in 2,879 Korean women with regular menstruation. *Korean J of Obstet Gynecol* 2012;**12**:920.

Legoff L, Dali O, D'Cruz SC, Suglia A, Gely-Pernot A, Hemery C, Kernanec PY, Demmouche A, Kervarrec C, Tevosian S *et al.* Ovarian dysfunction following prenatal exposure to an insecticide, chlordecone, associates with altered epigenetic features. *Epigenetics Chromatin* 2019;**1**:29.

Levine ME, Lu AT, Chen BH, Hernandez DG, Singleton AB, Ferrucci L, Bandinelli S, Salfati E, Manson JE, Quach A *et al.* Menopause accelerates biological aging. *Proc Natl Acad Sci U S A* 2016;**33**:9327–9332.

Levine ME, Lu AT, Quach A, Chen BH, Assimes TL, Bandinelli S, Hou L, Baccarelli AA, Stewart JD, Li Y *et al.* An epigenetic biomarker of aging for lifespan and healthspan. *Aging* 2018;**4**:573–591.

Liu K, Case A, Cheung AP, Sierra S, AlAsiri S, Carranza-Mamane B, Case A, Dwyer C, Graham J, Havelock J *et al.* Advanced reproductive age and fertility. *J Obstet Gynaecol Can* 2011;**11**:1165–1175.

Lu AT, Seeboth A, Tsai P-C, Sun D, Quach A, Reiner AP0, Kooperberg C, Ferrucci L, Hou L *et al.* DNA methylation-based estimator of telomere length. *Aging* 2019;**11**:5895–5923.

Marioni RE, Shah S, McRae AF, Chen BH, Colicino E, Harris SE, Gibson J, Henders AK, Redmond P, Cox SR *et al.* DNA methylation age of blood predicts all-cause mortality in later life. *Genome Biol* 2015;**25**:1–12.

McNatty K, Smith D, Makris A, Osathanondh R, Ryan K. The microenvironment of the human antral follicle: interrelationships among the steroid levels in antral fluid, the population of granulosa cells, and the status of the oocyte in vivo and in vitro. *J Clin Endocrinol Metab* 1979;**66**:851–860.

Morin SJ, Tao X, Marin D, Zhan Y, Landis J, Bedard J, Scott RT, Seli E. DNA methylation-based age prediction and telomere length in white blood cells and cumulus cells of infertile women with normal or poor response to ovarian stimulation. *Aging* 2018;**12**:3761–3773.

Natale MRD, Soch A, Ziko I, De Luca SN, Spencer SJ, Sominsky L. Chronic predator stress in female mice reduces primordial follicle numbers: implications for the role of ghrelin. *J Endocrinol* 2019;**3**:201–219.

Niu L, Xu Z, Taylor JA. RCP: a novel probe design bias correction method for Illumina methylation BeadChip. *Bioinformatics* 2016;**17**: 2659–2663.

OECD Family database. Age of mothers at childbirth and age-specific fertility 2018. http://www.oecd.org/els/family/database.htm.

Olesen MS, Starnawska A, Bybjerg-Grauholm J, Bielfeld AP, Agerholm I, Forman A, Overgaard MT, Nyegaard M. Biological age of the endometrium using DNA methylation. *Reproduction* 2018;**2**:167–172.

Pan JX, Tan YJ, Wang FF, Hou NN, Xiang YQ, Zhang JY, Liu Y, Qu F, Meng Q, Xu J *et al.* Aberrant expression and DNA methylation of lipid metabolism genes in PCOS: a new insight into its pathogenesis. *Clin Epigenetics* 2018;**6**:1–12.

Parisi S, McKay MJ, Molnar M, Thompson MA, van der Spek PJ, van Drunen-Schoenmaker E, Kanaar R, Lehmann E, Hoeijmakers JHJ, Kohli J. Rec8p, a meiotic recombination and sister chromatid cohesion phosphoprotein of the Rad21p family conserved from fission yeast to humans. *Mol Cell Biol* 1999;**5**:3515–3528.

Perna L, Zhang Y, Mons U, Holleczek B, Saum KU, Brenner H. Epigenetic age acceleration predicts cancer, cardiovascular, and all-cause mortality in a German case cohort. *Clin Epigenetics* 2016;**64**:1–7.

Peters TJ, Buckley MJ, Statham AL, Pidsley R, Samaras KV, Lord R, Clark SJ, Molloy PL. De novo identification of differentially methylated regions in the human genome. *Epigenetics Chromatin* 2015;**1**:1–16.

Phipson B, Maksimovic J, Oshlack A. missMethyl: an R package for analysing methylation data from Illuminas HumanMethylation450 platform. *Bioinformatics* 2015;**2**:286–288.

Qu F, Wang FF, Yin R, Ding GL, El-Prince M, Gao Q, Shi BW, Pan HH, Huang YT, Jin M *et al.* A molecular mechanism underlying ovarian dysfunction of polycystic ovary syndrome: hyperandrogenism induces epigenetic alterations in the granulosa cells. *J Mol Med (Berl)* 2012;**8**:911–923.

R Core Team. A Language and Environment for Statistical Computing 2016.

Rajpert-De Meyts E, Jørgensen N, Græm N, Müller J, Cate RL, Skakkebæk NE. Expression of anti-Mullerian hormone during normal and pathological gonadal development: association with differentiation of Sertoli and granulosa cells. *J Clin Enocrinol Metab* 1999;**10**: 3836–3844.

Rakyan VK, Down TA, Maslau S, Andrew T, Yang TP, Beyan H, Whittaker P, McCann OT, Finer S, Valdes AM *et al.* Human aging-associated DNA hypermethylation occurs preferentially at bivalent chromatin domains. *Genome Res* 2010;**4**:434–439.

Regan SLP, Knight PG, Yovich JL, Arfuso F, Dharmarajan A. Growth hormone during in vitro fertilization in older women modulates the density of receptors in granulosa cells, with improved pregnancy outcomes. *Fertil Steril* 2018;**7**:1298–1310.

Roy S, Gandra D, Seger C, Biswas A, Kushnir VA, Gleicher N, Kumar TR, Sen A. Oocyte-derived factors (GDF9 and BMP15) and FSH regulate AMH expression via modulation of H3K27AC in granulosa cells. *Endocrinology* 2018;**9**:3433–3445.

Rödström K, Bengtsson C, Milsom I, Lissner L, Sundh V, Bjoürkelund C. Evidence for a secular trend in menopausal age: a population study of women in Gothenburg. *Menopause* 2003;**6**:538–543.

Sagvekar P, Kumar P, Mangoli V, Desai S, Mukherjee S. DNA methylome profiling of granulosa cells reveals altered methylation in genes regulating vital ovarian functions in polycystic ovary syndrome. *Clin Epigenetics* 2019;**1**:61.

Sanders JL, Newman AB. Telomere length in epidemiology: a biomarker of aging, age-related disease, both, or neither? *Epidemiol Rev* 2013;**35**:112–131.

Sawyer HR, Smith P, Heath DA, Juengel JL, Wakefield SJ, McNatty KP. Formation of ovarian follicles during fetal development in sheep. *Biol Reprod* 2002;**4**:1134–1150.

Scalercio SR, Brito AB, Domingues SF, Santos RR, Amorim CA. Immunolocalization of growth, inhibitory, and proliferative factors involved in initial ovarian folliculogenesis from adult common squirrel monkey (Saimiri collinsi). *Reprod Sci* 2015;**1**:68–74.

Scheffer GJ, Broekmans FJM, Looman CWN, Blankenstein M, Fauser BCJM, DeJong FH, Te Velde ER. The number of antral follicles in normal women with proven fertility is the best reflection of reproductive age. *Hum Reprod* 2003;**4**:700–706.

Sehl ME, Henry JE, Storniolo AM, Ganz PA, Horvath S. DNA methylation age is elevated in breast tissue of healthy women. *Breast Cancer Res Treat* 2017;**1**:209–219.

Shammas MA. Telomeres, lifestyle, cancer, and aging. *Curr Opin Clin Nutr Metab Care* 2011;**1**:28–34.

Silver MJ, Kessler NJ, Hennig BJ, Dominguez-Salas P, Laritsky E, Baker MS, Coarfa C, Hernandez-Vargas H, Castelino JM, Routledge MN et al. Independent genomewide screens identify the tumor suppressor VTRNA2-1 as a human epiallele responsive to periconceptional environment. *Genome Biol* 2015;**118**:1–14.

Simpkin AJ, Howe LD, Tilling K, Gaunt TR, Lyttleton O, McArdle WL, Ring SM, Horvath S, Smith GD, Relton CL. The epigenetic clock and physical development during childhood and adolescence: longitudinal analysis from a UK birth cohort. *Int J Epidemiol* 2017;**2**:549–558.

Statistics Denmark. The register of 'FOD11: Average age of women given birth and new fathers' 2018. https://www.statbank.dk/FOD11.

Teschendorff AE, Menon U, Gentry-Maharaj A, Ramus SJ, Weisenberger DJ, Shen H, Campan M, Noushmehr H, Bell CG, Maxwell AP et al. Age-dependent DNA methylation of genes that are suppressed in stem cells is a hallmark of cancer. *Genome Res* 2010;**4**:440–446.

The Danish Fertility Society. *Annual Report 2018: 'The results for 2018 are based on reports from public as well as private fertility clinics to the Danish Health Authority's IVF register'*. 2019. Danish Fertility Society. https://fertilitetsselskab.dk/dataark-pr-aar/.

Titus S, Li F, Stobezki R, Akula K, Unsal E, Jeong K, Dickler M, Robson M, Moy F, Goswami S et al. Impairment of BRCA1-related DNA double-strand break repair leads to ovarian aging in mice and humans. *Sci Transl Med* 2013;**172**: 172ra121.

Tsutsumi M, Fujiwara R, Nishizawa H, Ito M, Kogo H, Inagaki H, Ohye T, Kato T, Fujii T, Kurahashi H. Age-related decrease of meiotic cohesins in human oocytes. *PLOS ONE* 2014;**5**:e96710.

Van Noord PAH, Boersma H, Dubas JS, Te Velde E, Dorland M. Age at natural menopause in a population-based screening cohort: the role of menarche, fecundity, and lifestyle factors. *Fertil Steril* 1997;**1**:95–102.

Weidner CI, Lin Q, Koch CM, Eisele L, Beier F, Ziegler P, Bauerschlag DO, Jockel K-H, Erbel R, Muhleisen TW et al. Aging of blood can be tracked by DNA methylation changes at just three CpG sites. *Genome Biol* 2014;**2**:R24.

Westergaard CG, Byskov AG, Andersen CY. Morphometric characteristics of the primordial to primary follicle transition in the human ovary in relation to age. *Hum Reprod* 2007;**8**:2225–2231.

Wissing ML, Kristensen SG, Andersen CY, Mikkelsen AL, Høst T, Borup R, Grøndahl ML. Identification of new ovulation-related genes in humans by comparing the transcriptome of granulosa cells before and after ovulation triggering in the same controlled ovarian stimulation cycle. *Hum Reprod* 2014;**5**:997–1010.

Xu Z, Langie SA, De Boever P, Taylor JA, Niu L. RELIC: a novel dye-bias correction method for Illumina methylation BeadChip. *BMC Genomics* 2017;**1**:4.

Xu Z, Niu L, Li L, Taylor JA. ENmix: a novel background correction method for Illumina HumanMethylation450 BeadChip. *Nucleic Acids Res* 2016;**3**:e20.

Yu B, Russanova V, Gravina S, Hartley S, Mullikin J, Ignezweski A, Graham J, JH S, AH DC, Howard B. DNA methylome and transcriptome sequencing in human ovarian granulosa cells links age-related changes in gene expression to gene body methylation and 3′-end GC density. *Oncotarget* 2015;**6**:3627–3643.

Zhang D, Zhang X, Zeng M, Yuan J, Liu M, Yin Y, Wu X, Keefe DL, Liu L. Increased DNA damage and repair deficiency in granulosa cells are associated with ovarian aging in rhesus monkey. *J Assist Reprod Genet* 2015;**7**:1069–1078.

Zoubarev A, Hamer KM, Keshav KD, McCarthy EL, Santos JR, Van Rossum T, McDonald C, Hall A, Wan X, Lim R et al. Gemma: a resource for the reuse, sharing and meta-analysis of expression profiling data. *Bioinformatics* 2012;**17**:2272–2273.